A tri-atomic Renner-Teller system entangled with Jahn-Teller conical intersections

A. Csehi, A. Bende, G. J. Halász, Á. Vibók, A. Das et al.

Citation: J. Chem. Phys. **138**, 024113 (2013); doi: 10.1063/1.4773352
View online: http://dx.doi.org/10.1063/1.4773352
View Table of Contents: http://jcp.aip.org/resource/1/JCPSA6/v138/i2
Published by the American Institute of Physics.

A tri-atomic Renner-Teller system entangled with Jahn-Teller conical intersections

A. Csehi,[1] A. Bende,[2] G. J. Halász,[1] Á. Vibók,[3] A. Das,[4] D. Mukhopadhyay,[4] and M. Baer[5,a)]

[1]*Department of Information Technology, University of Debrecen, H-4010 Debrecen, P.O. Box 12, Hungary*
[2]*Molecular and Biomolecular Physics Department, National Institute for Research and Development of Isotopic and Molecular Technologies, Cluj-Napoca, Romania*
[3]*Department of Theoretical Physics, University of Debrecen, H-4010 Debrecen, P.O. Box 5, Hungary*
[4]*Department of Chemistry, University of Calcutta, Kolkata 700 009, India*
[5]*The Fritz Haber Research Center for Molecular Dynamics, The Hebrew University of Jerusalem, Jerusalem 91904, Israel*

(Received 8 September 2012; accepted 11 December 2012; published online 14 January 2013)

The present study concentrates on a situation where a Renner-Teller (RT) system is entangled with Jahn-Teller (JT) conical intersections. Studies of this type were performed in the past for contours that surround the RT seam located along the collinear axis [see, for instance, G. J. Halász, Á. Vibók, R. Baer, and M. Baer, J. Chem. Phys. **125**, 094102 (2006)]. The present study is characterized by planar contours that intersect the collinear axis, thus, forming a unique type of RT-non-adiabatic coupling terms (NACT) expressed in terms of Dirac-δ functions. Consequently, to calculate the required adiabatic-to-diabatic (mixing) angles, a new approach is developed. During this study we revealed the existence of a novel molecular parameter, η, which yields the coupling between the RT and the JT NACTs. This parameter was found to be a pure number $\eta = 2\sqrt{2}/\pi$ (and therefore independent of any particular molecular system) and is designated as Renner-Jahn coupling parameter. The present study also reveals an unexpected result of the following kind: It is well known that each (complete) group of states, responsible for either the JT-effect or the RT-effect, forms a Hilbert space of its own. However, the entanglement between these two effects forms a third effect, namely, the RT/JT effect and the states that take part in it form a different Hilbert space. © *2013 American Institute of Physics*. [http://dx.doi.org/10.1063/1.4773352]

I. INTRODUCTION

This article is one additional link in a series of articles[1–4] devoted to the problem of revealing rigorous, efficient, and accurate methods to construct diabatic potential energy surfaces (PES) for multi-state, poly-atomic molecular systems. In the past, most of such articles were devoted to the calculation of diabatic PESs for limited regions in configuration space (CS), mainly, planar contours[5–12] (see also a list of studies in Ref. 4). Extending the available approaches to the required chemical volume, so that studies of chemical processes can be facilitated, was and still a formidable task. The main difficulty is associated with the single-valuedness of these diabatic PESs, which is difficult to guarantee even for simple CSs such as planes once they extend to large sizes. The severity of this issue increases significantly if one is interested in studying chemical exchange processes that require two or more arrangement channels.

Recently, while studying the HHF system, we managed to overcome, partially, this difficulty by introducing an approximate approach that fulfills two basic requirements: (a) It yields single-valued diabatic potentials for an arbitrary large plane; (b) it is rigorous in the sense that it originates from the Born-Oppenheimer (BO) treatment.[13,14] This approximation is based on complementary contours and by activating it we calculated planar PESs for the HHF system for a (R, θ) grid (see Fig. 1) covering the range $2.8 < R < 10$ a.u. and $-\pi/2 < \theta < +\pi/2$, respectively.[4] The planes under consideration are formed by the three atoms (a fluorine and two hydrogens in our case) and are parameterized via values of r, the inter-atomic distance of H_2. The (R, θ) grid points describe the polar coordinates of the F-atom with respect to the center-of-mass of the H_2 molecule on that plane.

In the present article, we consider a more advanced approach which is expected to yield diabatic PESs with higher accuracy.[3] It is based on three (or more) interacting states and therefore requires treating the adiabatic-to-diabatic transformation (ADT) matrices, A(**s**),[5,12] rather than the ordinary ADT (mixing) angles, γ(**s**) (see Eq. (1) in Ref. 4). As is well known, the literature contains numerous studies based on these matrices in connection with various different, tri-atomic, tetra-atomic, and poly-atomic molecular systems.[6(a),9,11,15,16(a),17,18] These studies are divided into two general categories based on the type of non-adiabatic coupling terms (NACT) included in the study: (a) ADT matrices formed by Jahn-Teller (JT) NACTs;[6(a),9,11,15] (b) ADT matrices formed by a mixture of both Renner-Teller (RT) NACTs and JT NACTs.[16(a),17,18(b),18(c)] This partitioning is somewhat artificial (in particular the existence of "pure" JT NACTs)

a)Email: michaelb@fh.huji.ac.il.

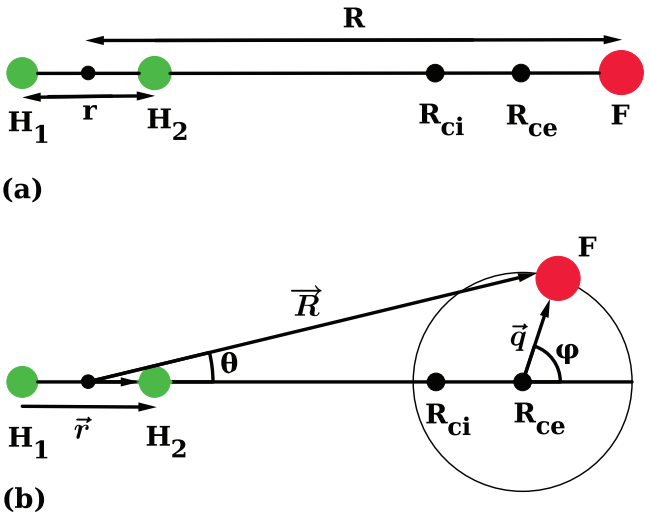

FIG. 1. A schematic picture of the system of coordinates: (a) Positions of atoms, point of (1,2) *ci* and the center of all circular contours. (b) System of coordinates: (R,θ|r) vs. (φ,q|r). In this figure, atoms F, H_1, and H_2 stand for atoms A, B, and C, respectively, mentioned in the text.

because molecular systems always contain both types of NACTs.

Since our aim is deriving diabatic PESs for the required chemical volume we have to guarantee that the approach to be developed treats the two kinds of NACTs. This was achieved in the just mentioned studies[16(a),17,18(b),18(c)] in which the ADT matrices are calculated employing line integrals along contours that surround the collinear axis, where the NACTs matrices contain both the RT and the JT NACTs (see also Ref. 16(b)).

The main shortcoming of this approach is that the ADT matrices are calculated for grids on a series of planes perpendicular to the collinear axis instead for the required grid on the tri-atomic plane. (We remind the reader that dynamical treatments are carried out on tri-atomic planes.) In other words, this approach demands intricate transformations from these numerous grids to the tri-atomic grid—a process that severely complicates the dynamical treatment (may be makes it even, altogether, infeasible). In what follows, we suggest calculating the ADT matrices for the tri-atomic grid directly. Another reason for this choice is that, for each value of the vibrational coordinate r, such a plane contains all JT *ci*s as well as the collinear axis that contains all RT degeneracy points and therefore the corresponding planar grid points are exposed to all the topological effects.

However, there is still one hurdle to overcome. Since all contours are assumed to be in the plane no contour is capable to surround this axis (which is in the plane) and therefore a different way to include the RT effect has to be found. Based on our past experience[19–21] a trustful way to include the RT effect is to let the contours intersect the degeneracy line and in this way to enable the corresponding NACT matrix elements to pick up the resulting RT effect. The only problem encountered here is that these calculated NACTs are extremely spiky—reminiscent of the Dirac δ-function (see, e.g., Fig. 2 in Ref. 21(a))—and therefore their correct shape is frequently missed.

This situation opened up the way for a theoretical/mathematical study according to which these NACTs are indeed, up to a normalization factor, pure Dirac δ-functions.[19,21(b)] The theoretical findings of this study are incorporated in the present study (see Eqs. (11a) and (11b)).

The article is arranged in the following way: In Sec. II is given the theoretical background which concentrates on the NACT matrices (for the tri-state and the tetra-state cases), on the corresponding extended (privileged) two-state ADT (mixing) angles and finally refers to the derivation of the Renner-Jahn parameter η,[3] in Sec. III are presented the calculations and in Sec. IV is given the discussion and summary of the results. We also mention Appendix A which briefly discusses the connection between the original Renner theory and the present RT NACT.

II. THEORETICAL BACKGROUND

A. Introductory remarks

Our approach is based on solving the following multi-dimensional first order differential equation:[5,12]

$$\nabla \mathrm{A}(\mathbf{s}) + \boldsymbol{\tau}(\mathbf{s})\mathrm{A}(\mathbf{s}) = \mathbf{0}, \tag{1}$$

where $\mathbf{A}(\mathbf{s})$, as previously mentioned, is the ADT matrix, $\tau(\mathbf{s})$ is an anti-symmetric matrix that contains the above mentioned vectorial NACTs and $\mathbf{s}$ is a variable that presents the collection of internal nuclear coordinates. The matrix $\boldsymbol{\tau}(\mathbf{s})$, which frequently contains singular elements, appears (together with the adiabatic, diagonal PES, $\mathbf{u}(\mathbf{s})$) in the nuclear Schrödinger equation (SE) following the BO treatment.[13,14] One way to avoid these singularities is to eliminate the $\boldsymbol{\tau}(\mathbf{s})$-matrix and form a modified SE free of all singularities but governed by $\mathbf{V}(\mathbf{s})$, a full potential matrix, which replaces the original, diagonal matrix, $\mathbf{u}(\mathbf{s})$. The two potential matrices are related via the following transformation:[5,12]

$$\mathbf{V}(\mathbf{s}) = \mathbf{A}(\mathbf{s})^{\dagger}\mathbf{u}(\mathbf{s})\mathbf{A}(\mathbf{s}), \tag{2}$$

where $\mathbf{A}(\mathbf{s})^{\dagger}$ is the complex conjugate matrix of $\mathbf{A}(\mathbf{s})$. The matrix $\mathbf{V}(\mathbf{s})$ is known as the diabatic PES—its diagonal elements are the corresponding diabatic potentials and its off diagonal elements form the diabatic coupling terms (reminiscing of the NACTs).

The common way to solve Eq. (1) is to assume contours, Γ, and to integrate it along such contours. Since $\mathbf{V}$(s) has to be presented at a given grid of points we must guarantee that the chosen contours (along which $\mathbf{A}(\mathbf{s})$ and $\mathbf{V}(\mathbf{s})$, are calculated) cover efficiently the full corresponding CS. While doing that we face again the troublesome singularities of the matrix $\boldsymbol{\tau}(\mathbf{s})$ which are also known as points of conical intersections (*ci*). These *ci*s may cause the diabatic potential $\mathbf{V}$(s) to be multi-valued (namely, non-single-valued) and therefore, essentially, of no physical use. To overcome this difficulty, the $\mathbf{A}$-matrix (which, according to Eq. (2), is responsible for the single-valuedness of $\mathbf{V}$(s)) has to be calculated employing numerous (usually 3-4) states so that upon completion of any closed contour in that CS it ends up as a diagonal matrix.[22]

A different way to treat these matrices is as follows: Since $\mathbf{A}$(s) is an orthogonal matrix it can be presented in terms of

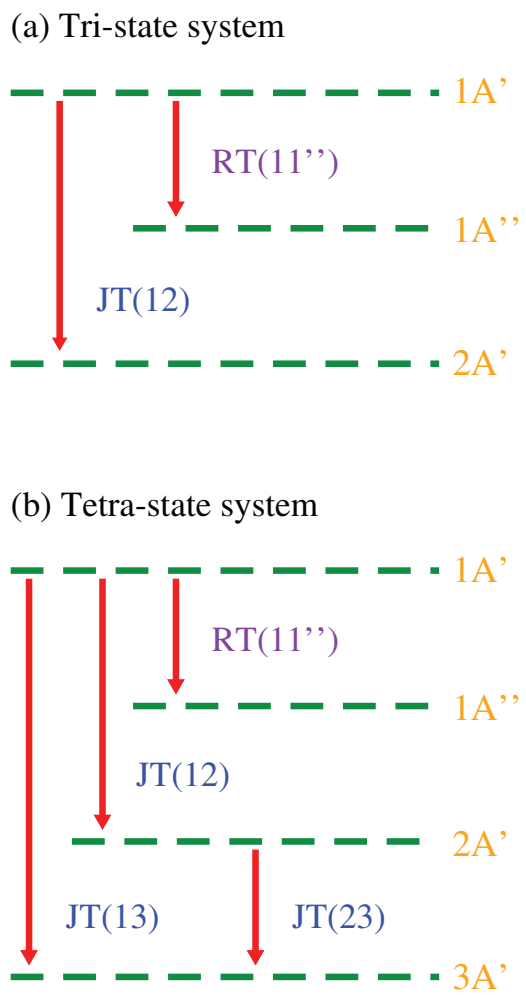

FIG. 2. Schematic figures describing the two RT/JT models: (a) the tri-state RT/JT model; (b) the tetra-state RT/JT model.

Euler kind of angles[18,23] and consequently its diagonality is guaranteed if and only if these angles, at the end of a closed contour, become integer multiples of π.[18(a),23(b)]

So far we referred to CSs in general but the above mentioned planar CSs are the ones to be considered for our purposes. (These planar CSs are, at a later stage, extended to form the full required chemical CS.) We remind the reader that in these planes the JT *cis* appear as isolated points and the RT degeneracy is located along the collinear tri-atomic axis which, obviously, is contained in the same plane (see Fig. 1).

B. Molecular states and the NACT matrix

Returning now to the last paragraph of the Introduction our aim is to construct NACT-matrices, $\boldsymbol{\tau}(\mathbf{s})$, which contain the two types of NACTs: the JT NACTs and the RT NACTs. This will be done for two molecular situations: (i) A system of three states, two A′-state and one A″-state (see Fig. 2(a)); (ii) a system of four states, three A′ and one A″ (see Fig. 2(b)).

1. Tri-state NACT-matrix

Here, the coupling between 1A′ and 2A′ is of the JT-type and designated as τ_{12} and the coupling between 1A′ and 1A″ is of the RT-type and designated as $\tau_{11''}$ (see Fig. 2(a)). We remind the reader that the two states 1A′ and 1A″ form a RT degeneracy line along the collinear HHF axis.

The NACT-matrix takes the form

$$\boldsymbol{\tau}(\mathbf{s}) = \begin{pmatrix} 0 & \tau_{11''} & \tau_{12} \\ -\tau_{11''} & 0 & 0 \\ -\tau_{12} & 0 & 0 \end{pmatrix}, \tag{3}$$

where we assumed that $\tau_{21''} \equiv 0$.

However, this form is not well suited for the numerical treatment as will be elaborated next. For reasons of convenience, we prefer to have τ_{12} at the (1,2) position of $\boldsymbol{\tau}(\mathbf{s})$. To achieve this arrangement, we permute between the last two rows and then between the last two columns so that $\boldsymbol{\tau}(\mathbf{s})$ becomes

$$\boldsymbol{\tau}(\mathbf{s}) = \begin{pmatrix} 0 & \tau_{12} & \tau_{11''} \\ -\tau_{12} & 0 & 0 \\ -\tau_{11''} & 0 & 0 \end{pmatrix} \tag{3′}$$

which is the NACT-matrix of the desired form. It is important to mention that the solution of Eq. (1) is not affected by these permutations.

2. Tetra-state NACT matrix

Here, the NACTs between 1A′ and 2A′, between 1A′ and 3A′ and between 2A′ and 3A′ are of a JT-type, designated as $\boldsymbol{\tau}_{12}$, $\boldsymbol{\tau}_{13}$, and $\boldsymbol{\tau}_{23}$, respectively, and the coupling between 1A′ and 1A″ is, like before, of the RT-type and designated as $\tau_{11''}$ (see Fig. 2(b)).

The NACT-matrix takes form

$$\boldsymbol{\tau}(\mathbf{s}) = \begin{pmatrix} 0 & \tau_{11''} & \tau_{12} & \tau_{13} \\ -\tau_{11''} & 0 & 0 & 0 \\ -\tau_{12} & 0 & 0 & \tau_{23} \\ -\tau_{13} & 0 & -\tau_{23} & 0 \end{pmatrix}. \tag{4}$$

As in the previous case, this matrix is not well suited for our numerical treatment. Again for reason of convenience we prefer to have the six JT-NACTs to be concentrated in the upper 3 × 3 diagonal corner of the 4 × 4 matrix and the two RT-NACTs to be at the peripheral positions. To achieve this, we permute between the second and the third rows and then between the second and the third columns, so that $\boldsymbol{\tau}(\mathbf{s})$ becomes

$$\boldsymbol{\tau}(\mathbf{s}) = \begin{pmatrix} 0 & \tau_{12} & \tau_{11''} & \tau_{13} \\ -\tau_{12} & 0 & 0 & \tau_{23} \\ -\tau_{11''} & 0 & 0 & 0 \\ -\tau_{13} & -\tau_{23} & 0 & 0 \end{pmatrix}. \tag{4′}$$

Next, we permute between the two last rows and then between the two last columns so that $\boldsymbol{\tau}(\mathbf{s})$ becomes

$$\boldsymbol{\tau}(\mathbf{s}) = \begin{pmatrix} 0 & \tau_{12} & \tau_{13} & \tau_{11''} \\ -\tau_{12} & 0 & \tau_{23} & 0 \\ -\tau_{13} & -\tau_{23} & 0 & 0 \\ -\tau_{11''} & 0 & 0 & 0 \end{pmatrix} \tag{4″}$$

which is the NACT-matrix of the required form.

C. ADT matrices and privileged angles

1. Two-state case and the ADT angle

In the early days, we used to solve Eq. (1) by treating the full **A**-matrix as it stands without paying much attention to its internal structure. The only exceptional case is the two-state case where the **A**-matrix which can be expressed in terms of one angle $\gamma(s)$ (to be termed as the ADT or mixing angle) and this leads to the following simple line integral:[12]

$$\gamma_{12}(s|\Gamma) = \int_{s_0}^{s} ds' \cdot \tau_{12}(s'|\Gamma). \tag{5}$$

Here, τ_{12} was introduced earlier, Γ designates the contour along which is carried out the integration and the dot presents the scalar product. Since we intend to consider circular contours only the integration can be simplified to become over an angle, φ

$$\gamma_{12}(\varphi, q) = \int_0^{\varphi} \tau_{\varphi 12}(\varphi', q)d\varphi', \tag{6}$$

where (φ, q) are polar coordinates: q is the radius, φ is the angle associated with the (nuclear) rotation. Consequently, the corresponding angular component of τ_{12} is, as usual, presented in the form: $(1/q)\tau_{\varphi 12}(\varphi,q)$, where

$$\tau_{\varphi 12}(\varphi, q) = \left\langle \zeta_1(\mathbf{s}_e|\varphi, q) \left| \frac{\partial}{\partial\varphi} \zeta_2(\mathbf{s}_e|\varphi, q) \right\rangle \right. . \tag{7}$$

Here $\zeta_j(\varphi|q)$; $j = 1, 2$ are the corresponding eigenfunctions related to the two lower states (in our case the states $1^2A'$ and $2^2A'$). In addition to the ADT angle, we are also interested in the angle $\alpha_{12}(q)$—the-end-of-the-contour phase—defined as

$$\alpha_{12}(q) = \int_0^{2\pi} \tau_{\varphi 12}(\varphi', q)d\varphi' \tag{8}$$

and is known as the topological/geometrical phase.

Comment: About two decades ago it was suggested[24] to identify the topological phase with the Berry phase for a two-state system.[25] This connection was found to be valid for all reported numerical studies of molecular systems with two quasi-isolated states.[4,15–17,21(a),26–28]

In case the two-state system forms a Hilbert subspace the topological phase becomes an integer multiple of π (or zero). In the Introduction, we already mentioned that the necessary and sufficient condition that the diabatic potentials, formed by Eq. (2), are of physical value in a given region in CS is that the topological phase (see Eq. (8)) is equal to $n\pi$ (where n is an integer) for any closed contour in that region. In case the two-state topological phase is not equal to $n\pi$ in the considered region, we are forced to include three states or sometimes more to guarantee that the relevant topological phase(s) is(are) integer multiples of π. This will be done next.

2. Tri-state privileged angle

As already mentioned in the Introduction, we take advantage of the fact that $\mathbf{A}(\varphi,q)$ is a 3×3 orthogonal matrix and therefore its nine elements can be presented in terms of the three quasi-Euler angles.[18,23] This idea was already elaborated, applied, and analyzed in a series of articles[3,7,9,11,18,29,30] and, therefore, is only briefly discussed here.

As in case of the ordinary Euler matrix, the orthogonal **A**-matrix is presented as a product of three rotation matrices $\mathbf{Q}_{ij}(\gamma_{ij})$ $(i < j = 2, 3)$ where the product $\mathbf{A} = \mathbf{Q}_{kl}\mathbf{Q}_{mn}\mathbf{Q}_{pq}$ can be written in any order. Substituting this product in Eq. (1) yields three coupled first-order differential equations for the three corresponding quasi-Euler angles, γ_{ij}. The final set of equations as well as their solution depends on the order of the **Q**-matrices.[18(a)]

In an analysis carried out several years ago,[18(b),18(c),29] we attributed physical meaning only to one of the three ADT angles, γ_{ij}, privileged with an equation that contains the corresponding NACT, τ_{ij}, as a free isolated term (there is one equation like that in every group of three coupled equations). In what follows, we assume γ_{12} to be such an angle and consider for this purpose the product: $\mathbf{A} = \mathbf{Q}_{12}(\gamma_{12})\mathbf{Q}_{13}(\gamma_{13})\mathbf{Q}_{23}(\gamma_{23})$. Substituting this product in Eq. (1) yields three first order equations, of which two equations (for γ_{12} and γ_{13}) form a closed subgroup of two coupled equations[3]

$$\frac{\partial}{\partial\varphi}\gamma_{12} = -\tau_{12} - \tan\gamma_{13}(\tau_{23}\cos\gamma_{12} + \tau_{13}\sin\gamma_{12}), \tag{9a}$$

$$\frac{\partial}{\partial\varphi}\gamma_{13} = \tau_{23}\sin\gamma_{12} - \tau_{13}\cos\gamma_{12}. \tag{9b}$$

These two equations are solved with the aim of calculating the privileged ADT angle $\gamma_{12}(\varphi, q)$. The introduction of the privileged angle enables the extension of the earlier defined two-state topological phase, α_{12}, to three-state systems. A straightforward choice is the end-of-the-contour value of the angle γ_{12}. Thus, $\alpha_{12}(q) = \gamma_{12}(\varphi = 2\pi, q)$.

3. Tetra-state privileged angle

To treat the four-state case, we need to express the 4×4 **A**-matrix in terms of six quasi-Euler angles which implies—similar to the tri-state case—that **A** has to be presented as a product of six rotational matrices: $\mathbf{Q}_{ij}(\gamma_{ij})$ $(i < j = 2, 3, 4)$.[18(c),30] In this context we refer, again, to the corresponding privileged angle, γ_{12} and employ for this purpose the corresponding product of elementary rotational matrices[18(c)]

$$\mathbf{A} = \mathbf{Q_{12}Q_{13}Q_{14}Q_{23}Q_{24}Q_{34}} \Rightarrow \mathbf{Q_{ij}} = \mathbf{Q_{ij}}(\gamma_{ij}).$$

Substituting this product in Eq. (1) yields a group of six first-order differential equations (see Eq. (20) in Ref. 18(c)), of which the first three equations (for the angles γ_{12}, γ_{13}, and γ_{14}) form a closed subgroup of coupled equations

$$\nabla\gamma_{12} = -\tau_{12} - \tan\gamma_{13}(\tau_{13}\sin\gamma_{12} + \tau_{23}\cos\gamma_{12}) - \tan\gamma_{14}\sec\gamma_{13}(\tau_{14}\sin\gamma_{12} + \tau_{24}\cos\gamma_{12}), \tag{10a}$$

$$\nabla\gamma_{13} = \tan\gamma_{14}\sin\gamma_{13}(\tau_{24}\sin\gamma_{12} - \tau_{14}\cos\gamma_{12}) + \tau_{23}\sin\gamma_{12} - \tau_{13}\cos\gamma_{12} - \tau_{34}\tan\gamma_{14}\cos\gamma_{13}, \tag{10b}$$

$$\nabla\gamma_{14} = -\tau_{14}\cos\gamma_{12}\cos\gamma_{13} + \tau_{24}\sin\gamma_{12}\cos\gamma_{13} + \tau_{34}\sin\gamma_{13}. \tag{10c}$$

These three equations are solved with aim of calculating, $\gamma_{12}(\varphi,q)$, the privileged ADT angle and $\alpha_{12}(q)$, the corresponding topological phase, which, as before, is defined as the end-of-the-contour value of the angle γ_{12}, namely, $\alpha_{12}(q) = \gamma_{12}(\varphi = 2\pi, q)$.

D. The inclusion of the Renner-Teller effect

1. Presentation of the intra-planar RT NACT

Whereas the calculations of two-state JT-NACTs along circular contours, Γ, in the tri-atomic plane is well known we, mainly, concentrate on the RT-NACT, $\tau_{11''}$, along the same contour (see Sec. II B 1). As already mentioned earlier, we concentrate on circles that have their centers on the collinear axis. Since the collinear axis is an infinite long interval $-\infty < R < +\infty$ each such circle intersects this line at two points, i.e., at $\varphi = 0$ and at $\varphi = \pi$ (see Fig. 1(b)). It is well known that at each such intersection point, along a short interval perpendicular to the collinear axis, is formed a spiky non-zero NACT (in this case an angular NACT) with features reminiscent of a Dirac δ-function.[21(b),31] Thus, our first tendency is to assume that the angular RT-NACTs in the planar CS take the form[3]

$$\boldsymbol{\tau}_{11''}(\varphi|q,\Gamma) = \frac{\pi}{2}\delta(\varphi - \vartheta) \tag{11a}$$

for any circle Γ with a radius q (here ϑ designates the intersection points and is either zero or π—see Fig. 1(b)). Equation (11a) has to be applied with some care because as it stands it yields, for any circle, a quantized topological phase ($=\pi$) to be expected for an undisturbed RT effect along Γ. However, in Sec. II A we assumed the existence of a JT *ci* on the collinear axis and therefore the RT effect is most likely weakened (or, eventually, intensified) by this *ci*.[32] Consequently, the pure RT quantization is affected and a way to incorporate this possibility is to extend Eq. (11a) by adding a normalization factor, η, thus,

$$\boldsymbol{\tau}_{11''}(\varphi|q,\Gamma) = \frac{\pi}{2}\eta\delta(\varphi - \vartheta), \tag{11b}$$

where η (most likely ≤ 1) is a parameter to be determined theoretically. In what follows Eq. (11b) is termed as the quasi-Dirac δ-function and η is termed as the Renner-Jahn coupling parameter (RJCP). More about Eq. (11b) is given in Sec. IV.

Although the circular contour intersects the HHF axis at two points, namely, at $\varphi = 0, \pi$ we consider only what happens at $\varphi = \pi$. It can be shown that the RT-NACT at $\varphi = 0$ has no affect on the results.

2. The tri-state JT/RT coupled equations

In order to derive the corresponding differential equations for the tri-state RT/JT coupled system, we consider the NACT-matrix given in Eq. (3′) and substitute the relevant matrix elements in Eqs. (9a) and (9b). Thus,

$$\frac{\partial}{\partial\varphi}\gamma_{12}(\varphi) = -\tau_{12}(\varphi) - \tau_{11''}(\varphi)\tan\gamma_{13}(\varphi)\sin\gamma_{12}(\varphi), \tag{12a}$$

$$\frac{\partial}{\partial\varphi}\gamma_{13}(\varphi) = -\tau_{11''}(\varphi)\cos\gamma_{12}(\varphi), \tag{12b}$$

where the integration is done along a circular contour, and therefore the first-order differentiation operator ∇, is replaced by the angular derivative: $(\partial/\partial\varphi)$. Parts of Eqs. (12) can be integrated analytically taking advantage of Eq. (11b). Defining the following Heaviside step function:

$$\Theta(\varphi - \pi) = \begin{cases} 0; & 0 \leq \varphi \leq \pi \\ 1; & \pi \leq \varphi \leq 2\pi \end{cases}, \tag{13}$$

it can be shown that the solution of Eq. (12b) is proportional to this step function

$$\gamma_{13}(\varphi) = \Theta(\varphi - \pi)\gamma_{13}^{(0)}(\varphi), \tag{14a}$$

where

$$\gamma_{13}^{(0)}(\varphi) = -\eta\frac{\pi}{2}\cos\{\gamma_{12}(\varphi = \pi)\} \tag{14b}$$

and that the solution of Eq. (12a) is also a step function of a somewhat more involved form

$$\gamma_{12}(\varphi) = -\int_0^{\varphi} d\varphi'\tau_{12}(\varphi') + \Theta(\varphi - \pi)\chi(\varphi = \pi), \tag{15a}$$

where $\chi(\varphi = \pi)$ is given in the form

$$\chi(\varphi = \pi) = -\eta\frac{\pi}{2}\tan\left\{\gamma_{13}^{(0)}(\varphi = \pi)\right\}\sin\{\gamma_{12}(\varphi = \pi)\}. \tag{16}$$

Equation (16) is characterized by the following features: (i) In case $|\gamma_{12}(\varphi = \pi)| > \pi/2$ the sign of $\chi(\varphi = \pi)$ is opposite to the sign of $\gamma_{12}(\varphi = \pi)$, e.g., when $\gamma_{12}(\varphi = \pi) < 0$, then $\chi(\varphi = \pi) > 0$. (ii) In case $|\gamma_{12}(\varphi = \pi)| < \pi/2$, the sign of $\chi(\varphi = \pi)$ is identical to the sign of $\gamma_{12}(\varphi = \pi)$, e.g., when $\gamma_{12}(\varphi = \pi) < 0$, then $\chi(\varphi = \pi) < 0$.

For the whole approach to be meaningful the upward/downward vertical shifts, as expressed in terms of $\chi(\varphi = \pi)$, have to fulfill two conditions (see Appendix B for additional information)

(1) Since the diabatic potentials have to be single-valued at every point in CS they have to be so also at $\varphi = \pi$. Consequently, the value of $\chi(\varphi = \pi)$ has to guarantee the equality: $\sin[\gamma_{12}(\varphi = \pi)] = \sin[\gamma_{12}(\varphi = \pi) + \chi]$ and a similar equality (up to a sign) for the cosine function.

(2) Since the value of $\gamma_{12}(\varphi)$ at the end of the closed circular contour, namely, at $\varphi = 2\pi$ has to be $\gamma_{12}(\varphi = 2\pi) = \pm n\pi$ the vertical shift, $\chi(\varphi = \pi)$, has to guarantee the following quantization condition:

$$\alpha(q) = -\int_0^{2\pi} d\varphi'\tau_{12}(\varphi') + \chi(\varphi = \pi) = \pm n\pi, \tag{15b}$$

where $\alpha(q)$ is recognized as the relevant topological phase (see Eq. (8)).

In Sec. II D 4, these conditions will be discussed in more detail for the case of infinite small deviations.

3. The tetra-state JT/RT coupled equations

In what follows are derived the differential equations for the tetra RT/JT coupled system. For this purpose, we consider

the NACT-matrix given in Eq. (4″) (thus, τ_{24} and τ_{34} are identically zero and τ_{14} is replaced by $\tau_{11''}$) and substitute the relevant matrix elements in Eqs. (10a)–(10c). Thus,

$$\frac{\partial}{\partial\varphi}\gamma_{12} = -\tau_{12} - \tan\gamma_{13}(\tau_{13}\sin\gamma_{12} + \tau_{23}\cos\gamma_{12}) - \tau_{11''}\tan\gamma_{14}\sec\gamma_{13}\sin\gamma_{12}, \tag{17a}$$

$$\frac{\partial}{\partial\varphi}\gamma_{13} = \tau_{23}\sin\gamma_{12} - \tau_{13}\cos\gamma_{12} - \tau_{11''}\tan\gamma_{14}\sin\gamma_{13}\cos\gamma_{12}, \tag{17b}$$

$$\frac{\partial}{\partial\varphi}\gamma_{14} = -\tau_{11''}\cos\gamma_{12}\cos\gamma_{13}. \tag{17c}$$

Next, Eq. (17c) is integrated analytically taking advantage of Eq. (11b). Thus,

$$\gamma_{14}(\varphi) = \Theta(\varphi-\pi)\gamma_{14}^{(0)}(\varphi), \tag{18a}$$

where

$$\gamma_{14}^{(0)}(\varphi) = -\eta\frac{\pi}{2}\cos[\gamma_{12}(\varphi=\pi)]\cos[\gamma_{13}(\varphi=\pi)]. \tag{18b}$$

To continue we distinguish between the two intervals:

(i) $0 \le \varphi < \pi$. Along this interval $\gamma_{14}(\varphi) \equiv 0$ and we are left with following two equations (for γ_{12}, γ_{13}):

$$\nabla\gamma_{12} = -\tau_{12} - \tan\gamma_{13}(\tau_{13}\sin\gamma_{12} + \tau_{23}\cos\gamma_{12}), \tag{19a}$$

$$\nabla\gamma_{13} = \tau_{23}\sin\gamma_{12} - \tau_{13}\cos\gamma_{12}. \tag{19b}$$

These equations are solved for the initial conditions $\gamma_{12}(\varphi=0) = \gamma_{13}(\varphi=0) \equiv 0$.

It is interesting to emphasize that Eqs. (19a) and (19b) are identical to the set of equations which have to be solved for an ordinary system of three coupled JT states.

(ii) $\pi < \varphi \le 2\pi$. Along this interval are encountered the (same) equations as given by Eqs. (19a) and (19b) (because $\tau_{11''}(\varphi) \equiv 0$) but here $\gamma_{14}(\varphi)$, although being a constant, differs from zero (see Eqs. (18a) and (18b)). Equations (19a) and (19b) are, therefore, solved along the interval ($\varphi \ge \pi$), for the following initial conditions:

(I)

$$\gamma_{12}^{(0)}(\varphi=\pi) = \gamma_{12}(\varphi=\pi) + \chi_{12}(\varphi=\pi), \tag{20a}$$

where $\chi_{12}(\varphi=\pi)$ — the (1,2) vertical shift — is given as

$$\chi_{12}(\varphi=\pi) = -\frac{\pi}{2}\eta\tan\left\{\gamma_{14}^{(0)}(\varphi=\pi)\right\} \times \sin\{\gamma_{12}(\varphi=\pi)\}\sec\{\gamma_{13}(\varphi=\pi)\} \tag{21a}$$

and

(II)

$$\gamma_{13}^{(0)}(\varphi=\pi) = \gamma_{13}(\varphi=\pi) + \chi_{13}(\varphi=\pi), \tag{20b}$$

where $\chi_{13}(\varphi=\pi)$ — the corresponding (1, 3) vertical shift — is given in the form

$$\chi_{13}(\varphi=\pi) = -\frac{\pi}{2}\eta\tan\left\{\gamma_{14}^{(0)}(\varphi=\pi)\right\} \times \cos\{\gamma_{12}(\varphi=\pi)\}\sin\{\gamma_{13}(\varphi=\pi)\}. \tag{21b}$$

Corollary: Equations (21a) and (21b) indicate, unambiguously, that no shift takes place whenever $\gamma_{12}(\varphi=\pi) = \pi/2$. This conclusion is independent of the value RJCP, η.

4. Derivation of the Renner-Jahn coupling parameter η

To derive the RJCP, η, we consider the solution for $\gamma_{12}(\varphi)$ as given in Eq. (15a) for the case that $\gamma_{12}(\varphi)$ at $\varphi=\pi$ is slightly larger than $\pi/2$, namely,

$$\gamma_{12}(\varphi=\pi) = \pi/2 + \varepsilon. \tag{22}$$

Here, ε is a constant assumed to be small enough to guarantee the fulfillment of the required approximations. Substituting Eq. (22) in Eq. (16) yields for the corresponding vertical shift, $\chi(\varphi=\pi)$, the value[3]

$$\chi(\varphi=\pi) = \left(\eta\frac{\pi}{2}\right)^2\varepsilon. \tag{23}$$

Based on continuity we expect that, for $\varepsilon \to 0$, two requirements have to be fulfilled by $\chi(\varphi)$ at $\varphi=\pi$. We start with the single-valuedness for the diabatic potentials (see Appendix B for additional information) which is fulfilled when $\sin(\pi/2+\varepsilon) = \sin(\pi/2+\varepsilon-\chi)$ $\{\equiv\sin(\pi/2-\varepsilon)\}$. In other words, the single-valuedness is fulfilled when $(\pi/2+\varepsilon-\chi) = (\pi/2-\varepsilon)$ or $\chi(\varphi=\pi) = 2\varepsilon$. Recalling Eq. (23) we see that this happens when η is[3]

$$\eta = \frac{2\sqrt{2}}{\pi} = 0.9003. \tag{24}$$

We continue with the quantization requirement and for this purpose we employ Eq. (15b). From Eq. (22) we get, due to symmetry, that $\gamma_{12}(\varphi)$ at $\varphi=2\pi$ becomes $\pi+2\varepsilon$. Substituting this outcome in (16), we find that the quantization is fulfilled whenever $2\varepsilon-\chi=0$ thus, as before, this equality yields for η the result given in Eq. (23) and consequently also Eq. (24).

So far the η-value in Eq. (24) was determined for the case that $\varepsilon \to 0$ or when $\gamma_{12}(\varphi=\pi)$ is only slightly larger than $\pi/2$ (see Eq. (22)). In Ref. 3 we conducted, for the F + H_2 system, a numerical study with the aim of finding out to what extent this value of η applies also for arbitrary large shifts. Indeed, for all considered cases (even for vertical shifts up to $\sim$ 2 Rad.), we find the differences between the theoretical shifts and the required numerical ones to be negligibly small (see a comparison along the two last columns of Table 1 given in Ref. 3).

So far this derivation was carried out for the tri-state case. It can be shown that an identical result is obtained for the tetra-state case. In other words, the transition from a tri-state system to a tetra-state system leaves RJCP unaffected.

Comment: As already mentioned in the Introduction, we also studied systems affected by both, JT-NACTs and RT-NACTs[16(a),17,18] where the contours surround the RT seams (and therefore do not intersect them) so that the resulting RT NACTs are not of the Dirac δ-function type and the need for η-type parameters becomes redundant.

III. NUMERICAL RESULTS

A. Introductory comments

As mentioned earlier we apply the numerical treatment to the $H_2 + F$ system (the model described in Sec. II B is constructed to be suitable for this system). The $F + H_2$ system was treated by numerous groups during the last half-century but we mention here only the studies by Werner *et al.*[33,34] In particular, we refer to the numerical treatment by Stark and Werner[33(a)] who not only produced the up-to-date, ground state (adiabatic) potential for this system but also revealed the existence of a JT *ci* located on the collinear axis in vicinity of $R \sim 5.5$ a.u. (mentioned earlier while constructing the model) and derived the first diabatic potentials for this system (more details are given in Refs. 1, 2, and 4).

Our study is carried out for the planar CS as formed by assuming $r(= R_{HH})$ to be fixed at $r = 1.4$ a.u. (see Fig. 1).

In this treatment are calculated, employing MOLPRO,[33(b)] only JT-NACTs (see Appendix C for details) and the corresponding ADT angles. For this purpose are considered the three lowest states of type A′ coupled at three collinear (JT) *ci*-points: the (1,2) *ci*-point is located at the vicinity of $R = R_{ci} \sim 5.5$ a.u.;[33(a)] the (2,3) *ci*-point located at the vicinity of $R = R_{ci} \sim 1.9$ a.u. and the (3,4) *ci*-point located at the vicinity of $R = R_{ci} \sim 1.8$ a.u. (see Fig. 1). In this respect, we mention that the (1,2)*ci* is formed by a Σ-state, assigned as 2A′ and one of the two Π-states (with the same symmetry) assigned as 1A′ (see Fig. 2).

As mentioned earlier the RT degeneracy is formed by two Π-states, designated as 1A′ and 1A″ (see Fig. 2) and, as usual, are located along the (collinear) HHF axis. The corresponding RT-NACTs required for the present study are not calculated but assumed to be quasi-Dirac-δ functions as discussed in Sec. II D.

The calculations and the theoretical study are done (as frequently mentioned) along closed circular contours. All circles have their centers at the same fixed point on the collinear axis at $R = R_c = 6$ a.u. This common center is chosen in such a way as to guarantee that the various circles (with the varying radii) cover the whole planar CS of interest.

B. JT-NACTs along closed circles

In Fig. 3 are presented angular JT-NACTs as calculated along four different (closed) circles with the radii: q = 0.4, 3.0, 3,7, 4.0 a.u. In panel (a) is presented one NACT, namely, $\tau_{12}(\varphi|q = 0.4$ a.u.) whereas in all other panels we present three NACTs, namely, $\boldsymbol{\tau}_{12}(\varphi|q)$, $\boldsymbol{\tau}_{13}(\varphi|q)$, $\boldsymbol{\tau}_{23}(\varphi|q)$ (that couple the three lower A′ states) calculated along circles with larger radii: q = 3.0, 3.7, 4.0 a.u. The feature that characterizes the NACTs for q = 0.4 a.u. is that the circle does not surround the point of *ci* which is located at a distance of 0.5 a.u. from the center of the circle. In all other cases, the circles surround the *ci*-point and therefore the various $\boldsymbol{\tau}_{12}(\varphi|q > 0.5$ a.u.)'s exhibit a slightly more complicated structure. As for the two NACTs that couple the third state the following can be said: (a) $\boldsymbol{\tau}_{13}(\varphi|q)$ hardly changes as q increases; (b)

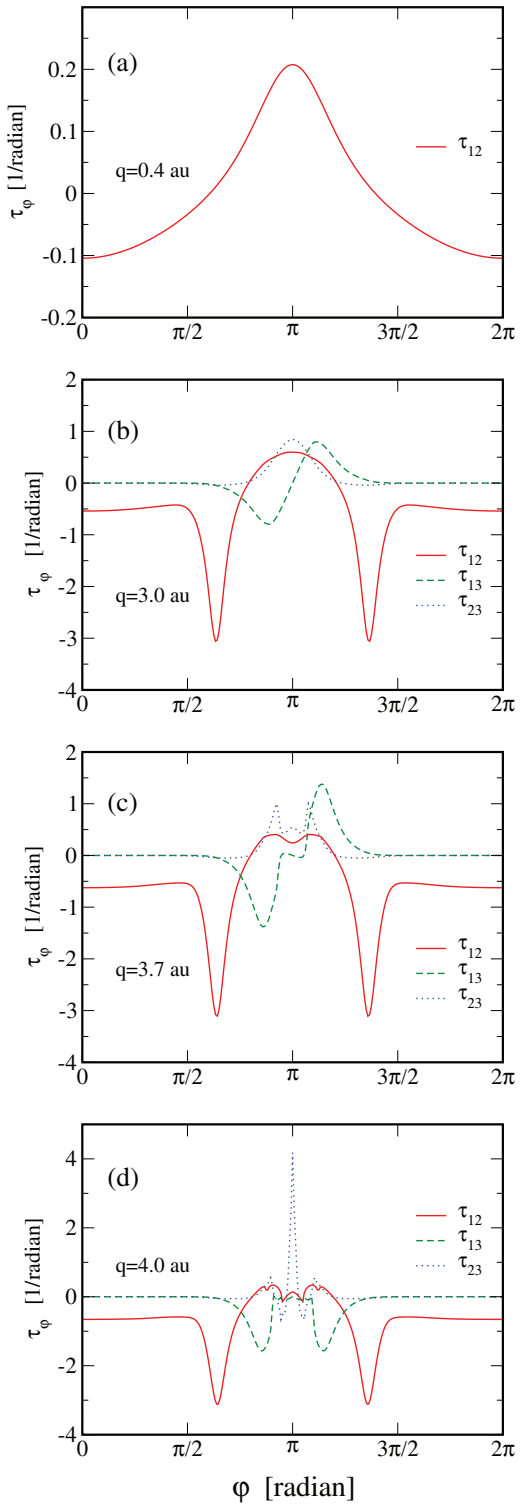

FIG. 3. Angular NACTs, $\tau_\varphi(\varphi|q)$, for circular contours at $R = R_{ce} = 6$ a.u. along the interval $0 \le \varphi \le 2\pi$: (a) $\tau_{12\varphi}(\varphi|q)$, for q = 0.4 a.u.; (b) $\tau_{12\varphi}(\varphi|q)$, $\tau_{13\varphi}(\varphi|q)$ and $\tau_{23\varphi}(\varphi|q)$, for q = 3 a.u.; (c) the same as in (b) but for q = 3.7 a.u.; (d) the same as in (b) but for q = 4 a.u.

$\boldsymbol{\tau}_{23}(\varphi|q)$ changes significantly and becomes spikier. The reason is associated with the fact that at $\{R \sim 1.8$ a.u., $\theta = 0\} \equiv \{q \sim 4.2$ a.u., $\varphi = \pi\}$ (see Fig. 1)) are located two additional JT *ci*s (as already mentioned earlier): a (2,3)*ci* and a (3,4)*ci*. As a result, the more remote is the center of the circle from these *ci*s the spikier (as a function of φ) is the corresponding NACT, $\boldsymbol{\tau}_{23}(\varphi|q)$. These spiky NACTs may lead to inaccuracies in calculating the corresponding ADT angles.

C. (1,2) ADT angles along closed circles

1. Tri-state results

In Fig. 4 are presented the (vertical) shifted (1,2) ADT angles, $\gamma_{12}(\varphi|q)$, as calculated according to the recipe in Eqs. (15a) and (16). Curves for nine q-values in the range $0.4 < q < 5.0$ a.u. are given. We distinguish between three types of curves: (1) The curve for $q = 0.4$ a.u. is not shifted (in other words, the shift is zero) and its topological phase, $\alpha_{12}(q)$, is zero which results from the fact that the circle does not surround the (1,2)*ci*. (2) The curve for $q = 1.0$ a.u. is not shifted (or the shift is negligible small) and is characteristic for the situation that the circle surrounds the (1,2)*ci* and therefore yields: $\alpha_{12}(q) = \pi$. (3) In all other cases, the circles surround the (1,2) *ci* and are shifted downwards (at $\varphi = \pi$). These two facts are the reason that all the topological phases $\alpha_{12}(q)$ are correctly quantized (namely, become equal to π when $\varphi = 2\pi$). At this stage, we emphasize again that the downwards shifts for the various cases were calculated according to formula in Eq. (16) (see, also, Eq. (14b)) where η is given by Eq. (24) and $\gamma_{12}(\varphi = \pi|q)$ is the corresponding privileged ADT angle. In other words, no artificial fitting is done!

Figure 4 reveals one interesting (and important) feature: The φ-dependence of the various curves become similar and the curves are converging to each other as the radius, q, of the circles increases. This phenomenon is general but is enhanced in the interval of $\pi/2 < \varphi < 3\pi/4$. Figure 5 shows, schematically, the region in CS — in the shape of a square — where the convergence is most efficient. As it happens this is the region where the chemical reaction takes place. In other words, it overlaps with the transition region from the reagents arrangement to the products arrangement.

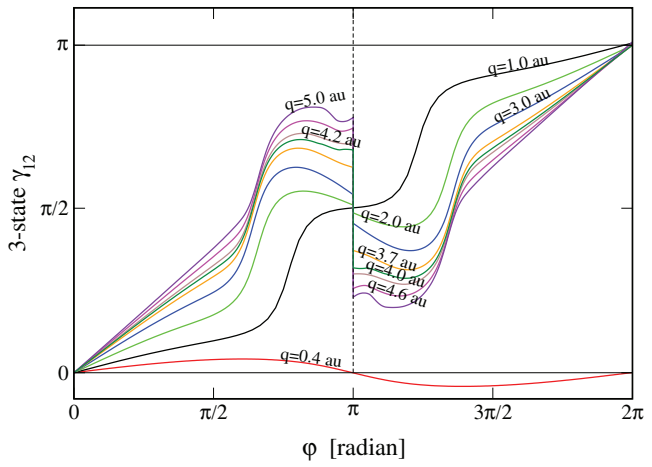

FIG. 4. The tri-state ADT (mixing) angle, $\gamma_{12}(\varphi|q)$, for circular contours at $R = R_{ce} = 6$ a.u. along the interval $0 \le \varphi \le 2\pi$ as calculated employing the RT/JT Eqs. (15a) and (16). Results are shown for q = 0.4, 1.0, 2.0, 3.0, 3.7, 4.0, 4.6, 5.0 a.u.

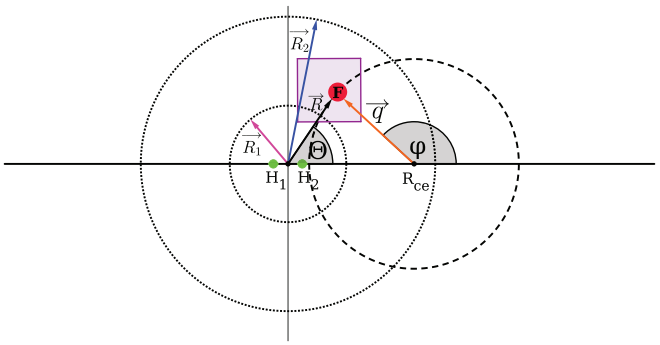

FIG. 5. The transition region, presented as a square, from reagents channel to products channel.

2. Tetra-state results

In Fig. 6 is presented a comparison between privileged ADT angles, $\gamma_{12}(\varphi|q)$ as calculated, once employing three states (see Eqs. (15a) and (16)) and once employing four states (see Eqs. (19)–(21)). These ADT angles are calculated along circles with the following radii: q = 3.0, 3.7, 4.0 a.u. presented in the relevant panels. As is noticed the results are well converged for all three cases. The encouraged fact from this comparison is that although the tetra-state ADT angles are calculated using two additional NACTs, namely, $\tau_{13}(\varphi|q)$ and $\tau_{23}(\varphi|q)$ (and therefore are based on more involved expressions to calculate the shifts at $\varphi = \pi$ — see Eqs. (20) and (21) — still, the ADT angles, are reasonably well converged.

IV. DISCUSSION AND CONCLUSIONS

In this article is studied the privileged, ADT angle $\gamma_{12}(\varphi|q)$ due to two entangled NACTs—the JT-NACT and the RT-NACTs. This was not the situation when we started studying the FHH system.[1,2] At that stage we employed one JT-NACT, namely, $\tau_{12}(\varphi|q)$, and following Eq. (6), we got quantized topological angles, $\alpha_{12}(q)$, only along circles with small radii ($q < 2.0$ a.u.). To improve the quantization for circles with larger radii ($q > 2.0$ a.u.), we added another A′-state as well as its two corresponding NACTs, $\boldsymbol{\tau}_{13}(\varphi|q)$ and $\boldsymbol{\tau}_{23}(\varphi|q)$, and solved Eqs. (19a) and (19b) — the relevant equations for the three-state JT situation (solved with the *initial* conditions: $\gamma_{12}(\varphi = 0) = \gamma_{13}(\varphi = 0) \equiv 0$). In Fig. 7 are compared the two JT-ADT angles $\gamma_{12}(\varphi|q)$, as calculated for $q = 4.0$ a.u. (once by solving Eq. (6) and once by Eqs. (19a) and (19b)). It is well noticed that the two kinds of calculations yield similar values for the topological phases, $\alpha_{12}(q)$ but which differ significantly from π. In other words, increasing the JT sub-Hilbert space from two states to three did not yield the expected quantization (unlike in numerous other cases[27,29]).

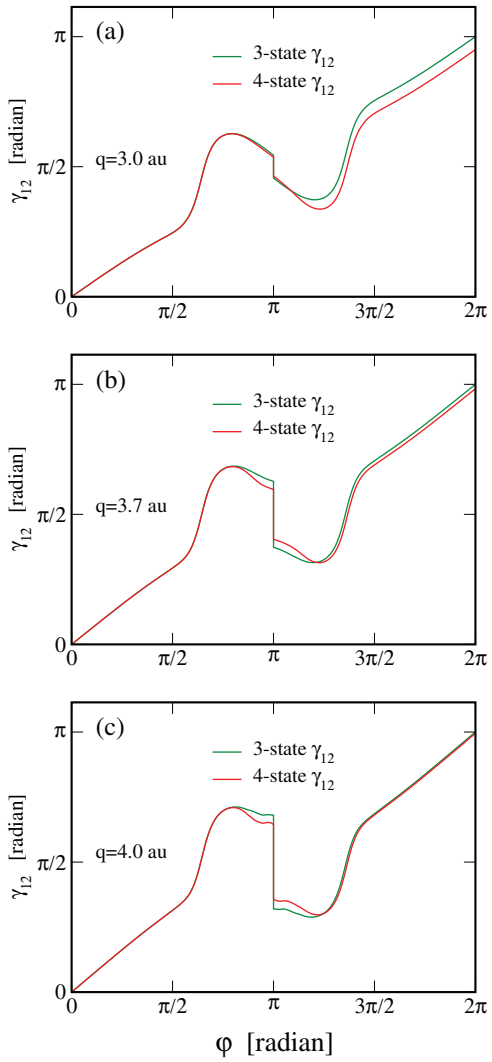

FIG. 6. A comparison between tri-state and tetra-state ADT (mixing) angles $\gamma_{12}(\varphi|q)$, for circular contours at $R = R_{ce} = 6$ a.u. along the interval $0 \leq \varphi \leq 2\pi$. The tri-state angles were calculated employing the RT/JT Eqs. (15a) and (16) and the tetra-state angles were calculated employing the RT/JT Eqs. (19a)–(21b). The comparison is presented in panel (a) for q = 3.0 a.u., in panel (b) for q = 3.7 a.u. and in panel (c) for q = 4.0 a.u.

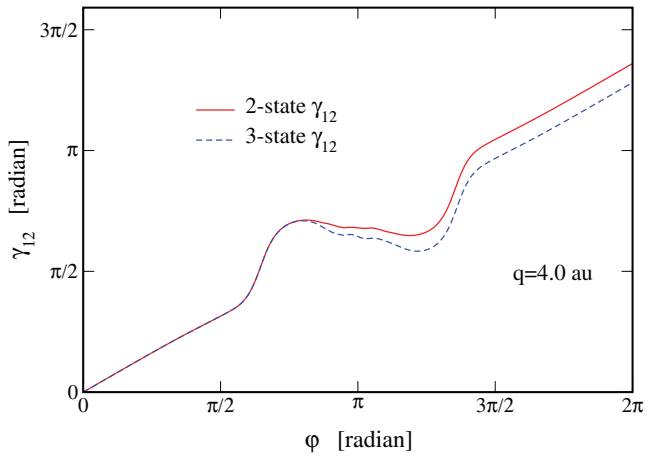

FIG. 7. ADT (mixing) angles, $\gamma_{12}(\varphi|q)$, calculated for a circular contour at $R = R_{ce} = 6$ a.u. with radius q = 4.0 a.u., along the interval $0 \leq \varphi \leq 2\pi$: Two JT curves are shown: a two-state curve calculated with Eq. (6) and a three-state curve calculated with Eqs. (19a) and (19b).

This fact led to the conclusion that the sharp increase of $\gamma_{12}(\varphi|q)$ in the region of $\pi/2 < \varphi < 3\pi/4$ is not caused by the existence of additional JT-*cis* (between higher states) but due to another factor, eventually, the RT-degeneracy which is formed between the two Π-states. To test this possibility, we developed a new methodology which enabled the numerical study of the entangled RT/JT system. This entangled system lent itself from the start to yield the desired improvement in the quantization (a feature required for guaranteeing single-valued diabatic PESs[1,2]).

The methodology presented here was introduced about a year ago,[3] for a tri-state system, and revealed the existence of a novel molecular parameter, η, responsible for the intra-planar coupling between the RT and the JT NACTs. This parameter was found to be a pure number $\eta = 2\sqrt{2}/\pi$ (= 0.9003). At the start we expected η to be dependent on the NACTs which would make it system dependent. So far the parameter η was not studied for other systems but the fact that the theoretical derivation yields a pure number implies that η is, probably, a kind of a universal molecular constant, at least as far as tri-atomic systems are concerned. This conclusion is further supported by the fact that an identical value for η is obtained for a tetra-state system.

The present study revealed an additional result: It is well known that each (complete) group of states responsible for one of the two effects, namely, the RT effect and the JT effect, forms an independent Hilbert space. However, most likely the entanglement (or engagement) between these two effects forms a third effect, namely, the RT/JT effect and the group of states responsible for it belongs to a more extensive Hilbert space.

Another aspect revealed in this study is that JT effects are not produced by conical intersections as in the ordinary case but by more elaborated intersections. This finding will be further studied in forthcoming publications.

As a final subject we refer to an issue which is frequently raised and expressed in different ways, for instance, "no unique solution exists for ADT matrices unless the number of states is ∞"[9] or how one overcomes the lack of a "closed sub-Hilbert space" in molecular systems, etc. Our answer is usually based on Mathematics and can be summarized in one word: Convergence. But this is not always sufficient as convergence might be attained for a non-physical situation (see, for example, in the first paragraph of this section and Fig. 7). In our field of research, we demand convergence to a meaningful physical limit and this implies attaining quantized phases. Thus, the idea is to increase the number of electronic states (which belong to an infinite large Hilbert space) until this goal is reached, namely, quantized phases along any closed contour in the region of interest. We can see that such a goal was reached in Fig. 6 when the number of states is increased from 3 to 4 (see Sec. III C 2).

Coming back to the authors in Ref. 9 (who demand an infinite number of states), their incriminating statements cannot be considered seriously as they did not deliver any details of their study (neither the number of states nor the size of configuration space used) that led them to draw their negative conclusions. Unfortunately, general statements of this kind cannot be productive.

ACKNOWLEDGMENTS

This work was partially supported by the Romanian National Authority for Scientific Research (ANCS) through the PN-II-RU-TE-2011-3-0124 Research Project. A.B. gratefully acknowledges the Data Center of NIRDIMT Cluj-Napoca for providing the computational infrastructure and the technical assistance. A.V. acknowledges the computational resources provided by the John-von-Neumann Institute, Research Centre Juelich (Project ID ehu01) and the OTKA (NN103251). The publication was supported by the TÁMOP-4.2.2.C-11/1/KONV-2012-0001 project. The project has been supported by the European Union, co-financed by the European Social Fund. M.B. would like to thank Professor R. Englman, from the Soreq Nuclear Research Center, Yavne, Israel for a discussion during which the possibility of the formation of a third effect, namely, the RT/JT effect, was considered for the first time.

APPENDIX A: THE RENNER THEORY AND THE RENNER-TELLER NACT

In 1934, Renner published a detailed study of a linear poly-atomic molecule, originally, characterized by the z-component of the electronic orbital angular momentum $\Lambda\hbar$ (where $\Lambda \neq 0$) and by a nuclear angular momentum component, $\ell\hbar$, associated with the bending vibrations of the molecule, both defined with respect to the molecule axis (considered to be the z-axis).[35] To be more specific, in this study Renner concentrated on those states that split to become two (coupled) states when moving away from collinearity. Thus, if we consider, e.g., a Π-state characterized by the quantum number $\Lambda = 1$ and a single eigenfunction, $\zeta_{\Lambda=1}(\mathbf{s}_e|\mathbf{s})$, then, after moving away from collinearity, one encounters two eigenfunctions, namely, $\zeta^{\pm}_{\Lambda=1}(\mathbf{s}_e|\mathbf{s})$ related to the two decoupled states (in this notation $\mathbf{s}_e$ and $\mathbf{s}$ stand for the collective electronic and nuclear coordinates, respectively).

Taking this model one step further and assuming the deviation from collinearity to be small enough (thus, the coordinate $\mathbf{s}$ is removed only slightly from the collinear arrangement) it is expected that the following result still holds:

$$\mathbf{L}^{(\pm)}_{z\Lambda=1}(\mathbf{s}) = \left\langle \zeta^{+}_{\Lambda=1}(\mathbf{s}_e|\mathbf{s}) \right| \mathbf{L}_z \left| \zeta^{-}_{\Lambda=1}(\mathbf{s}_e|\mathbf{s}) \right\rangle \sim -i\frac{1}{q}\Lambda(=1). \tag{A1}$$

Based on transformation between space fixed and body-fixed coordinates[36] one can show that in fact the z-component of the nuclear angular momentum operator $\mathbf{R}$, i.e., $\mathbf{R}_z$ can be expressed in terms of the associated nuclear angular coordinate φ, namely,

$$\mathbf{L}^{(\pm)}_{z\Lambda=1}(\mathbf{s}) \sim \mathbf{R}^{(\pm)}_{z\Lambda=1}(\mathbf{s}) = -i\frac{1}{q}\left\langle \zeta^{+}_{\Lambda=1}(\mathbf{s}_e|\mathbf{s}) \right| \frac{\partial}{\partial\varphi} \left| \zeta^{-}_{\Lambda=1}(\mathbf{s}_e|\mathbf{s}) \right\rangle. \tag{A2}$$

It is well noticed that Eq. (A2) is an expression reminiscent of the BO treatment and can be identified with rotational NACT as presented in Eq. (7).

To complete this presentation, we mention that recently Zhou *et al.*[37] employed the expression in Eq. (A1) in their dynamical study of the $N + H_2$ system.

APPENDIX B: THE DIABATIC POTENTIALS EXPRESSED IN TERMS OF ADT (MIXING) ANGLE

The diabatic potentials are given in the form[38]

$$\begin{aligned} V_1(\varphi|q) &= u_1(\varphi|q)\cos^2\gamma_{12}(\varphi|q) + u_2(\varphi|q)\sin^2\gamma_{12}(\varphi|q), \\ V_2(\varphi|q) &= u_1(\varphi|q)\sin^2\gamma_{12}(\varphi|q) + u_2(\varphi|q)\cos^2\gamma_{12}(\varphi|q), \\ V_{12}(\varphi|q) &= (1/2)\left(u_2(\varphi|q) - u_1(\varphi|q)\right)\sin\left(2\gamma_{12}(\varphi|q)\right), \end{aligned} \tag{B1}$$

where u_1 and u_2 are the adiabatic potentials, γ_{12} is ADT angle, and q and φ are the polar coordinates in the tri-atomic plane (see Fig. 1). A similar set of equations will hold for any other planar angles, e.g., (R,θ)—see Fig. 1.

APPENDIX C: THE NUMERICAL TREATMENT

The calculation of the NACTs (along chosen circles) was carried out at the state-average complete active space self-consistent field (CASSCF) level using the MOLPRO program.[33(b)] Within this calculation we used all seven valence electrons distributed on eight orbitals. Six electronic states, including the two/three studied states, were computed by this method applying equal weights.

The active space is made up of the 3σ-6σ orbitals, 1π valence orbital, and one additional set of correlating π-orbitals. Care has been taken to avoid the swap of 2σ and 3σ orbitals during the optimization of the orbitals at the CASSCF level.[33(b)] The basis set employed are: (a) for the fluorine we applied s and p functions from the cc-pV5Z set and d and f functions from cc-pVQZ set augmented with diffuse s, p, d, and f functions; (b) for the hydrogens we employed s functions from the cc-pV5Z set and p and d functions from the cc-pVQZ set augmented with diffuse s and p functions.

[1] A. Das, D. Mukhopadhyay, S. Adhikari, and M. Baer, Chem. Phys. Lett. **517**, 92 (2011).
[2] A. Das, D. Mukhopadhyay, S. Adhikari, and M. Baer, Eur. Phys. J. D **65**, 373 (2011).
[3] A. Das, D. Mukhopadhyay, S. Adhikari, and M. Baer, Int. J. Quantum Chem. **112**, 2561 (2012).
[4] A. Das, T. Sahoo, D. Mukhopadhyay, S. Adhikari, and M. Baer, J. Chem. Phys. **136**, 054104 (2012).
[5] M. Baer, *Beyond Born-Oppenheimer: Electronic Non-Adiabatic Coupling Terms and Conical Intersections* (Wiley, Hoboken NJ, 2006), Sec. 1.3.
[6] *Conical Intersections: Electronic Structure, Dynamics and Spectroscopy*, edited by W. Domcke, D. R. Yarkony, and H. Köppel (World Scientific, Singapore, 2004); in particularly see: (a) D. R. Yarkony, p. 41; (b) H. Köppel, p. 175; (c) R. de Vivie-Riedle and A. Hofmann, p. 829.
[7] A. Kuppermann and R. Abrol, Adv. Chem. Phys. **124**, 283 (2002).
[8] T. Pacher, L. S. Cederbaum, and H. Köppel, Adv. Chem. Phys. **84**, 293 (1993).
[9] O. Godsi, C. R. Evenhuis, and M. A. Collins, J. Chem. Phys. **125**, 104105 (2006).
[10] G. J. Halász, M. Sindelka, N. Moiseyev, L. S. Cederbaum, and Á. Vibók, J. Phys. Chem. A **116**, 2636 (2011); G. J. Halász, Á. Vibók, M. Sindelka, N. Moiseyev, and L. S. Cederbaum, J. Phys. B **44**, 175102 (2011).
[11] V. C. Mota, P. J. S. B. Caridade, and A. J. C. Varandas, Int. J. Quantum Chem. **111**, 3776 (2011).
[12] M. Baer, Chem. Phys. Lett. **35**, 112 (1975).
[13] M. Born and J. R. Oppenheimer, Ann. Phys. (Leipzig) **84**, 457 (1927).
[14] M. Born and K. Huang, *Dynamical Theory of Crystal Lattices* (Oxford University Press, New York, 1954), Chap. IV.

[15]M. S. Kaczmarski, Y. Ma, and M. Rohlfing, Phys. Rev. B **81**, 115433 (2010); B. Sarker and S. Adhikari, Int. J. Quantum Chem. **109**, 650 (2009); H. Negae, Y. Nakitani, and Y. Koyama, Chem. Phys. Lett. **474**, 342 (2009); A. Sirjoosingh and S. Hammes-Schiffer, J. Phys. Chem. A **115**, 2367 (2011); S. Al-Jabour, M. Baer, O. Deeb, M. Liebscher, J. Manz, X. Xu, and S. Zilberg, *ibid.* **114**, 2991 (2010); M. Labuda, J. Gonzalez-Vazquez, M. Fernando, and L. Gonzalez, Chem. Phys. **400**, 165 (2012); A. K. Paul, S. Ray, D. Muk, and S. Adhikari, J. Chem. Phys. **135**, 034107 (2011); I. Ryb and R. Baer, *ibid.* **121**, 10370 (2004); M. Baer, T. Vertesi, G. J. Halász, Á. Vibók, and S. Suhai, Discuss. Faraday Soc. **127**, 337 (2004).

[16](a) G. J. Halász, Á. Vibók, R. Baer, and M. Baer, J. Chem. Phys. **125**, 094102 (2006); (b) See also D. R. Yarkony, *ibid.* **90**, 1657 (1989) who calculated RT/JT NACTs for the $(HNO)^+$ system but did not form ADT angles usually required for diabatization.

[17]G. J. Halász, Á. Vibók, D. K. Hoffman, D. J. Kouri, and M. Baer, J. Chem. Phys. **126**, 154309 (2007).

[18](a) A. Alijah and M. Baer, J. Phys. Chem. A **104**, 389 (2000); (b) A. Das, D. Mukhopadhyay, S. Adhikari, and M. Baer, J. Chem. Phys. **133**, 084107 (2010); (c) A. Das and D. Mukhopadhyay, J. Phys. Chem. A **116**, 1774 (2012).

[19]Z. H. Top and M. Baer, Chem. Phys. **26**, 1 (1977).

[20]M. Baer, G. Niedner, and J. P. Toennies, J. Chem. Phys. **91**, 4169 (1989); C. L. Liao, R. Xu, G. D. Flesh, M. Baer, and C. Y. Ng, *ibid.* **93**, 4818 (1990).

[21](a) C. Levy, G. J. Halász, Á. Vibok, I. Bar, Y. Zeiri, R. Kosloff, and M. Baer, J. Chem. Phys. **128**, 244302 (2008); (b) Int. J. Quantum Chem. **109**, 2482 (2009).

[22]M. Baer, J. Phys. Chem. A **104**, 3181 (2000); M. Baer, S. H. Lin, A. Alijah, S. Adhikari, and G. D. Billing, Phys. Rev. A **62**, 032506 (2000); Ref. 5, Sec. 2.1.3.3.

[23](a) Z. H. Top and M. Baer, J. Chem. Phys. **66**, 1363 (1977); (b) Ref. 5, Sec. 5.5.3.

[24]M. Baer and R. Englman, Mol. Phys. **75**, 293 (1992).

[25]M. V. Berry, Proc. R. Soc. London, Ser. A **392**, 45 (1984).

[26]D. R. Yarkony, J. Chem. Phys. **105**, 10456 (1996); P. Barragan, L. F. Errea, A. Macias, L. Mendez, A. Riera, J. M. Lucas, and A. Aguilar, *ibid.* **121**, 11629 (2004); E. S. Kryachko, Adv. Quantum Chem. **44**, 119 (2003); Z.-R. Xu, M. Baer, and A. J. C. Varandas, J. Chem. Phys. **112**, 2746 (2000); C. Hu, O. J. Sugino, and K. Watanebe, J. Chem. Phys. **135**, 074101 (2011); W. Skomorowski, F. Pawlowski, T. Korona, R. Moszinski, P. S. Zuckowski, and J. M. Hutson, J. Chem. Phys. **134**, 114109 (2011); H. J. Werner, B. Follmeg, and M. H. Alexander, *ibid.* **89**, 3139 (1988).

[27]A. M. Mebel, A. Yahalom, R. Englman, and M. Baer, J. Chem. Phys. **115**, 3673 (2001); G. J. Halász, Á. Vibók, A. M. Mebel, and M. Baer, *ibid.* **118**, 3052 (2003).

[28]A. Csehi, G. J. Halász, and Á. Vibók, Chem. Phys. Lett. **533**, 10 (2012); G. J. Halász and Á. Vibók, *ibid.* **494**, 150 (2010); Int. J. Quantum Chem. **111**, 342 (2011).

[29]T. Vertesi, E. Bene, Á. Vibók, G. J. Halász, and M. Baer, J. Phys. Chem. A **109**, 3476 (2005).

[30]B. Sarker and S. Adhikari, J. Phys. Chem. A **112**, 9868 (2008).

[31]Z. H. Top and M. Baer, Chem. Phys. **26**, 1 (1977) (see Appendix A).

[32]M. Baer, A. M. Mebel, and G. D. Billing, Int. J. Quantum Chem. **90**, 1577 (2002).

[33] (a) K. Stark and H.-J. Werner, J. Chem. Phys. **104**, 6515 (1996); (b) H.-J. Werner and P. J. Knowles, MOLPRO, version 2010.1, a package of *ab initio* programs, see http://www.molpro.net (with contributions from J. Almlöf *et al.*).

[34]M. H. Alexander, H.-J. Werner, and D. E. Manolopoulos, J. Chem. Phys. **109**, 5710 (1998); M. H. Alexander, D. E. Manolopoulos, and H. J. Werner, *ibid.* **113**, 11084 (2000).

[35]E. Renner, Z. Phys. **92**, 172 (1934).

[36]M. Peric and S. Peyerimhoff, Adv. Chem. Phys. **124**, 583 (2002).

[37]S. Zhou, Z. Li, D. Xie, S. Lin, and H. Guo, J. Chem. Phys. **130**, 184307 (2009).

[38]M. Baer, Adv. Chem. Phys. **49**, 191 (1982) (see p. 283); Ref. 21, Sec. 3.1.1.3.